PLATON –

Planning Process and Tool for Step-by-Step Conversion of the Conventional or Mixed Bus Fleet to a 100% Electric Bus Fleet

Deliverable 4.2: Efficient Simulation
Part of Milestone M3
Main work package WP 4.4 Simulation components

Due Date: December 31, 2019

Report term: January 1, 2019 – December 31, 2019

Funding code: 03EMEN17

Project term: January 1, 2018 – June 30, 2020

Editor: Mikhail Kovalyov, UIIP
Contributors: Gerfried Cebrat, EUC
Olaf Czogalla, ifak

Grant beneficiary of WP leader:
Institut für Automation und Kommunikation e.V.

Funding organisation of WP leader:
Bundesministerium für Verkehr und digitale Infrastruktur
Invalidenstraße 44
10115 Berlin

Contents

1 Introduction

The deliverable presents the results of the project work carried out by consortium partners in the WP 4.4: Simulation Component.

The results of WP 4.4 are focused on the implementation of the simulation component by which potential scenarios of electric bus deployment can be assessed.

The simulation component of the Platon Toolkit is developed to simulate any potential scenarios, i.e. properties of electric buses that have been identified to fulfil the requirements of public transport and energy storage devices with a defined capacity, as well as known operating costs, passenger transportation demands and energy demands, to be used as input data for the planning problem in the transition process from conventionally propelled public transport to fully electrically propelled buses. A detailed outline on essential functionalities of the transition process is given in Algin Czogalla et al. [3], Deliverable 2.2 and 3.2.

This deliverable is composed of three main chapters. After preliminary definition of the scenarios as use cases for simulation, the simulation method used in the predecessor project CACTUS is described for reference reasons. The subsequent chapter deals with improvements of the simulation methodology and its environment to achieve a higher efficiency of the approach. The deliverable is completed with a chapter on simulation based on the Monte-Carlo method for efficient optimization of factors by modification of selected variables.

2 The scenario as a use case for simulation

A scenario – which may also be referred to as application case, use case or deployment scheme- includes information about dynamic economical, technical, social and ecological characteristics of the transportation system under planning.

The scenarios characterisation includes the following aspects. For bus types on the market and battery types must be included the total cost of ownership including capital costs, operational costs and costs for recycling of materials.

The energy demand to be determined by simulations is an important operational cost factor, especially in countries of high energy costs, and high share of fossile energy sources in the energy mix, such as in Germany.

Further, the anticipated numbers of passengers to be transported between activity locations in the city, the anticipated public transportation demand is significant for the characterization of the simulation scenario. The determination of the dynamic bus energy consumption is a separate important problem, which was studied and partly solved in the earlier project CACTUS and which will be further tackled in this task.

The most modern data structures, database systems, data exchange architecture have been used to make the simulation efficient.

If some required data is not available or if its generation assumes employment of an analytical model of an unreasonable size, the data can be simulated by a random sampling technique similar to the Monte-Carlo method.

In order to keep the simulation process fast, different time (or event) scales can be applied depending on the specific purpose of the dynamic process to be simulated. If the process is a single bus run between two stations, then the time scale can be based on minutes or seconds, or even assuming continuous time. If the process includes all bus activities over a day, then it can be based on minutes or bus arrivals and departures from stations. If the process includes all activities of a transportation system over a month or a year, then it can be based on days.

3 The simulation method of CACTUS

Aforementioned energy consumption and transport problems were studied and partly solved in the earlier project CACTUS. Hence, an overview about the CACTUS simulation methodology is given at this point, which is followed by pointing out the improvements being developed by the PLATON project.

The method of simulation was chosen within the CACTUS project because it was neither possible to really investigate electric buses nor combinations of energy storage types (battery, ultra-capacitor, flywheel) and energy transmission types (conductive, inductive) which are partially not realized so far. The method of simulation helps to investigate such combinations.

The input data include transportation models like the transport network, the timetable, the road network, the topography as well as technical models like buses, energy storage and energy transmission systems.

Table 1 Algorithm of simulation process control

```
public interface Process {
    public void performSimulationStep(int time);
}

Process[] p;

for time from 0 to n do
    for i from 0 to (number_of_processes - 1)
        p[i].performSimulationStep(time);
```

The algorithm shows the fundamental approach in pseudo code by the help of the interface mechanism known from the Java programming language. Each process to be simulated has to implement the `Process` interface with the `performSimulationStep` method. The global timer `time` counts from 0 to n and calls every process by handling over the current value of the global timer. Each process has to decide what to do within the elapsed time step. The global timer always increases by equidistant time steps.

There are several basic processes to be simulated: moving the bus including acceleration and deceleration as well as battery charging and battery changing.

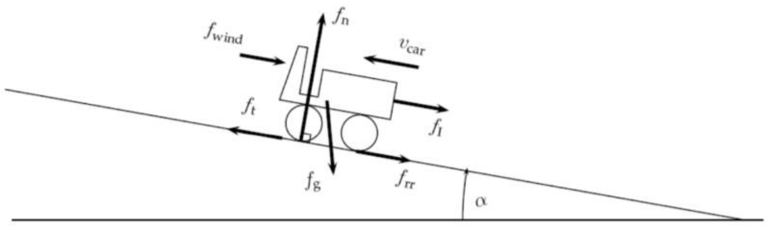

Figure 1 Forces acting on a car [11]

Starting at Figure 1and Equations (1.1) and 1.2 the energy for moving the bus -- depending on the speed, the acceleration and the rolling resistance of the tires, the wind, and the angle of the driving surface -- can be calculated. The traction force of a vehicle can be described by the following two equations [11]

$$F_t = \underbrace{M_{car}\dot{v}_{car}}_{f_I} + \underbrace{M_{car} \cdot g}_{f_g} \cdot \sin\alpha + \underbrace{\overbrace{sign(v_{car})M_{car} \cdot g \cdot \cos\alpha}^{f_n} \cdot c_{rr}}_{f_{rr}} + \underbrace{sign(v_{car} + v_{wind})\frac{1}{2}\rho_{air}C_{drag}A_{front}(v_{car} + v_{wind})^2}_{f_{wind}} \quad (1.1)$$

$$c_{rr} = 0.01\left(1 + \frac{3.6}{100}\right)v_{car} \quad (1.2)$$

where

F_t	$[N]$	Traction Force of the vehicle
f_I	$[N]$	Inertial force of the vehicle
f_{rr}	$[N]$	Rolling resistance force of the vehicle
f_g	$[N]$	Gravitational force of the vehicle
f_n	$[N]$	Normal force of the vehicle
f_{wind}	$[N]$	Force due to wind resistance
α	$[rad]$	Angle of the driving surface
M_{car}	$[kg]$	Mass of the vehicle
v_{car}	$[m/s]$	Velocity of the vehicle
$\dot{v}_{car}$	$[m/s^2]$	Acceleration of the vehicle
$g = 9.81$	$[m/s^2]$	Free fall acceleration
$\rho_{air} = 1.2041$	$[kg/m^3]$	Air density of dry air at 20 °C
c_{rr}	[-]	Tire rolling resistance coefficient
C_{drag}	[-]	Aerodynamic drag coefficient
A_{front}	$[m^2]$	Front area
v_{wind}	$[m/s]$	Headwind speed

The gradient of the way simply results from the elevations of the two successive locations on the run. Equation (1.4) calculates the gradient of the way in degrees, where Δh is the elevation difference between location one and location two and s is the distance between location one and location two.

$$\Delta h = h_{location1} - h_{location2} \tag{1.3}$$

$$\alpha = tan^{-1}\left(\frac{\Delta h}{s}\right) \tag{1.4}$$

Then the energy consumption over a period of time is calculated by the equations (1.5) and (1.6).

$$P = F_t \cdot v \tag{1.5}$$

$$E = \int P dt \tag{1.6}$$

where

P	$[W]$	Power
F_t	$[N]$	Traction Force
v	$[m/s]$	Speed
E	$[Ws]$	Energy consumption
dt	$[s]$	Period of time

The unit conversion is done by 1 kWh = 1.000 Wh = 3.600.000 Ws. This amount of energy is needed for moving the bus. The mass of the bus in [kg] includes the empty weight of the bus, the weight of the battery and the weight of the passengers.

Along the drivetrain from the battery to the wheels, energy losses occur. The electrical engine itself may have energy losses. The real energy consumption therefore is calculated by equation (1.7).

$$E_{total} = \eta_{Engine} \cdot E \tag{1.7}$$

The total energy consumption for moving the bus on a way between two successive bus stops is achieved by equation (1.8). It is the sum of the energy consumption of all time steps.

$$E_{Way} = \sum_{i=1}^{n} E_i \tag{1.8}$$

The remaining charging level of the energy storage after solving a way is simply calculated by equation (1.9).

$$E_{Battery} = E_{Battery} - E_{Way} \tag{1.9}$$

In order to come to more realistic viewpoint, the real speed profile must be considered which mostly is non-linear. Figure 2 depicts a speed-time diagram of a non-linear speed profile of a bus. The vertical lines within the diagram mark equal time periods. The default duration of such a time period is one second.

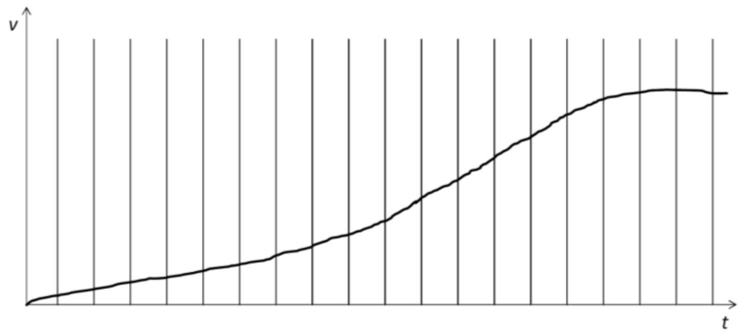

Figure 2 Speed-time diagram divided into several equal periods of time

When the bus decelerates, the waste energy can be recovered and stored back in the energy storage. The amount of energy to be recovered depends on the efficiency of the energy recovery unit. By the following equation, the amount of energy which is restored into the energy storage is calculated.

$$E(t) = \eta \cdot P \cdot \Delta t \tag{1.10}$$

Each engine (it does not matter whether electrical engine or Diesel engine) has energy losses and therefore an efficiency. The energy consumption really needed is higher than the energy calculated in equation (1.8). Therefore, it is calculated by the following equation (1.11) which considers the efficiency of the engine.

$$E_{total} = \frac{E_{Way}}{\eta_{Engine}} \tag{1.11}$$

Charging can be done while the bus is standing or while it is moving. We assume that the energy storage is being recharged simultaneously to consuming energy.

$$E(t) = \eta \cdot P \cdot \Delta t \tag{1.12}$$

with

E	[Ws]	Energy contained in the energy storage
η	[%]	Efficiency of energy transmission
P	[W]	Charging power
Δt	[s]	Energy transmission period of time

After charging, the charging level of the energy storage of the bus has increased by *E*. For example, charging with a power of 200 kW for a time period of 30 s results in 6000 kWs (or 1,66 kWh) by which the charging level rises. For simplification, a linear increase of the charging level of the energy storage is assumed.

The inventory comprises all parts of the bus which consume electrical energy excepting the engine. These parts belong to a conventional Diesel bus as well but in a Diesel bus the electrical energy needed is generated from the combustion engine. There are a lot of inventory devices within a bus in public transportation including air-conditioning, lighting, displays, ticket automat etc. to mention only the most important ones. Air-conditioning includes heating in winter and cooling in summer. It has the most energy consumption. We assume a continuous energy consumption of any device. That means we consider them as always on. The energy consumption can be calculated by the following equation (1.13):

$$E(t) = P_{Inventory} \cdot \Delta t \tag{1.13}$$

with

E	[Ws]	Energy consumption
$P_{Inventory}$	[W]	Power of the inventory
Δt	[s]	Working duration of the inventory

For example, the air condition may have a power of 900 W. For example, the lights may have a power of 500 W. The energy consumption of the inventory must be added to the energy consumption for moving the bus.

The main output value of the simulation is the energy consumption (for all considered bus routes) depending on the total mass of the bus, the speed profile and the elevation profile.

4 Architectural aspect of the PLATON simulation approach

The process of bus fleet electrification comprises all targeted efforts to introduce or increase the number of battery electric buses in fleets of local public transport agencies. Several domains are involved in these processes such as the legislative and governmental domain, the economic domain, the public transport domain and finally the electric power domain. Numerous dependencies exist between entities of the named domains which are described in detail by the authors but will be not further elaborated here.

However, for understanding of this highly dependent process it is essential to acknowledge that, derived from the interdependent relationships, there were identified multiple levels of the planning process itself. Therefore, exist a multi-layer structure of the planning process in the same sense, including bodies of stakeholders on these levels. At least three main level were distinguished, such as: i) the legislative-governmental level, ii) the strategic corporate planning level, and iii) the transport operations planning level.

Any set of tools, here named the *Toolkit*, designed to support the decision-making on these process levels i)-iii) is likely to function relatively autonomously with regard to each planning levels, but must be interoperable concerning data exchange with basic input data of the transport region of interest. An interface definition and documentation must contain not only the mathematical semantic description of the required input data contents but also the data model and data architecture in order to achieve the required interoperability.

For this reason, a dedicated Application and Data Architecture was derived and developed to ensure the interoperability and conformance to the dependency network as well as the distinguished planning levels that were identified. Interoperability is required to ensure a seamless data exchange between components of the PLATON Toolkit. There are numerous categories of data to be distinguished with respect to input data and output data. Input data is to be referred as the input to components of the toolkit. These can be output data of other tool components or data from open or proprietary sources. In Figure 3 is shown the information and data architecture between components of the PLATON Toolkit System.

The directed arcs between the green marked tool components represent flows of data objects from their source to their destination including the category and formats. Note that the planning levels addressed, are emphasized as strategic corporate planning level and transport operation planning level. Decision support will be provided in form of generated reports that comprise the most important output for strategic decisions such as TCO projection of the bus fleet, electrification priority of routes, procurement recommendation based on the configuration of vehicle, batteries and charging infrastructure.

More specific planning support is provided to the transport operations level such as scheduling for electric buses, opportunity charging locations or potential transit network adaptations with regard to the existing power grid under consideration of the transit demand.

The architecture reveals the data flow, interfaces and sources of data for the toolkit system which is developed to the extent of the shown information and data architecture in Figure 3 as of December 2019.

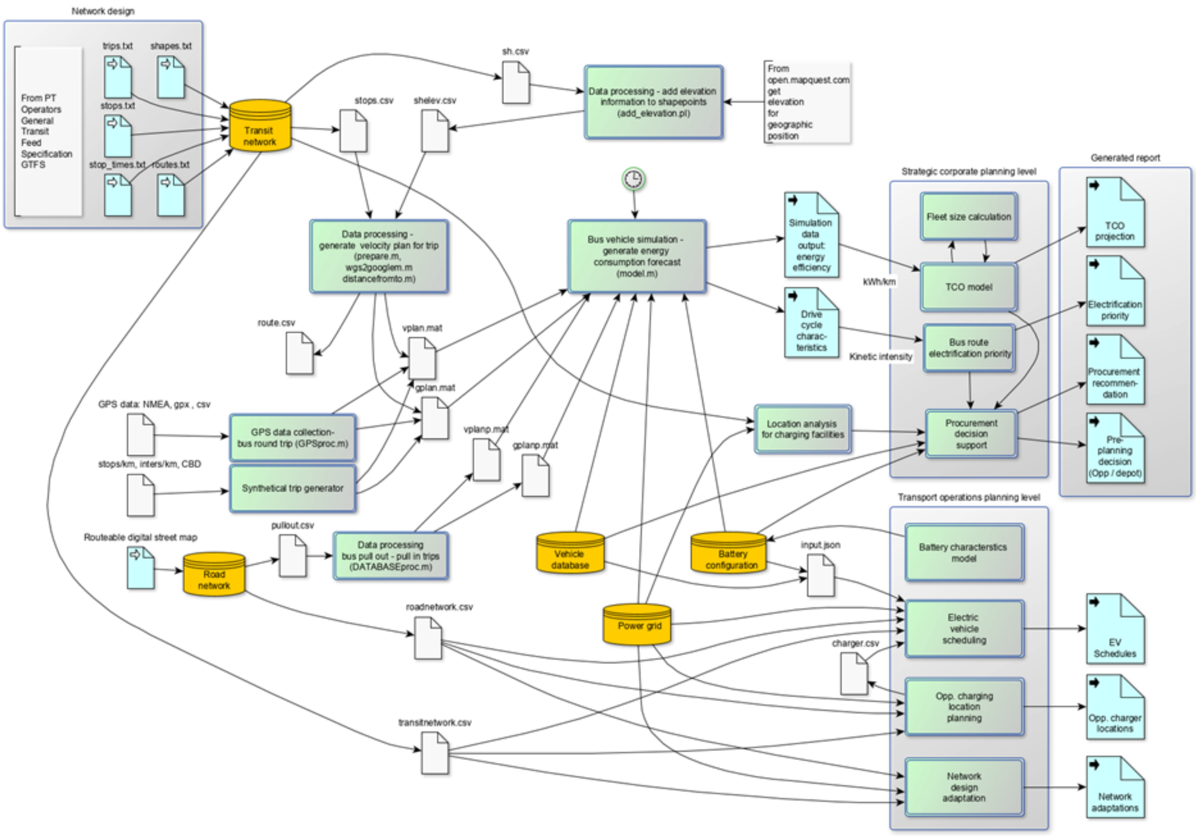

Figure 3 Information and data architecture of PLATON Toolkit System and its components

5 Improvements of simulation approach to advance efficiency

Essential improvements to the CACTUS approach to advance the efficiency are related to the Bus vehicle simulation component of Figure 3 that is connected to the realistic transit network of the considered scenario as well as to the vehicle database, battery configurations and the power grid, which are the input data sources.

Nearly all of the outlined tool components rely on geographical mapping data that represent the existing transit network covering the area that is serviced by the given transit agency. Ideally, the mapping data is available in an exchange format that enables seamless integration into each of the planning tools. A standardized data interface enables not only the exchange between planning tools as well as the application of the complete tool set in an arbitrary transit service area. Examples for such standard data interfaces are VDV 452 (Interface Network Timetable) [1] and Google's General Transit Feed Specification GTFS [2].

The GTFS specification was utilized in the present case to develop a workflow for data extraction to make this data source available for all tool components to be designed.

In Figure 3 is also shown the workflow to capture geographic data on shapes of route segments, stops, and assigned trips with stop times for the given timetable of the selected bus service. The data in text files are imported into a database to facilitate further processing and refinement. The internet based open *Mapquest* service is included into the workflow by a data processing application to add elevation information to the geographic shape coordinates. Information on elevation is essential to calculation of ascending or descending terrain grades along the bus route for simulation based energy consumption forecast.

In addition to the database approach, a direct field measurement application of GPS data was developed and implemented on the smartphone. By this component, all relevant input data including route shapes, elevation and stop locations are collected and processed for the bus vehicle simulator that was implemented in GNU Octave. The bus vehicle simulator was extended by a database of bus vehicle specifics including drivetrain, battery configurations and motor characteristics of current models from e-bus manufacturers (Volvo, Solaris, BYD, Mercedes, MAN, VDL, Iveco).

5.1 Electric bus vehicle model

The basic vehicle model was established as a tractive force model following Sun [4] in which the tractive force F_T equals the resistance forces like rolling resistance F_R due to tire and road resistance, wind resistance F_W due to air and vehicle interaction, grade resistance F_G due to the grades of the road, and acceleration resistance F_A due to accelerate the vehicle mass.

$$F_T = F_R + F_W + F_G + F_A \tag{2.1}$$

or

$$F_T = K_R \cdot m \cdot \cos(\theta) + K_W \cdot A \cdot v^2 + m \cdot \sin(\theta) + m \cdot \frac{a}{g} \tag{2.2}$$

with rolling resistance coefficient K_R, vehicle weight m, road angle θ in radians, wind resistance coefficient K_C, vehicle frontal area A, vehicle speed v, vehicle acceleration a and gravitational constant g. The characteristics of the simulated bus vehicle were obtained from manufacturer BYD and are listed inTable 2. For simulation, a fully loaded bus was assumed with a total number of 75 passengers (30 seats plus 45 standees) with an average passenger mass of 68 kg [9].

Table 2 Selected parameters of the simulated bus vehicle

Model/Make	Solaris Urbino 12 Electric
Mass/Load	13,790 kg / 5,100 kg
Frontal area	8.66 m²
Max. torque	973 Nm
Max. power	250 kW
Final gear drive ratio	22.6
Battery capacity	240 kWh
Voltage (open circuit)	600 V
Accessory load (HVAC)	5 kW

5.2 Driver and drivetrain model

In Figure 4 is shown a principal bus vehicle model that was used for simulation of longitudinal duty cycles of a fully loaded bus vehicle as described by given parameters. Acceleration and braking commands are the output of the PI controller. The output signal is normalized and limited to a unit less range between -1 and 1. Here, positive signal values from 0 to 1 are translated to accelerator pedal positions (APP), whereas negative signal values from -1 to 0 are translated to braking pedal positions (BPP). The positive APP signal is transferred by the proportional electric synchronous motor model into mechanical torque τ_{mot}. Braking pedal commands are translated to braking force F_b by factoring in the gross vehicle weight *m* and the maximum allowed deceleration of *a* = -1 m/s². The selected deceleration limit is in accordance with Standardised On-Road Test cycles (SORT) for public buses as standard for passenger comfort, such as defined in [12].

5.3 Vehicle dynamics

The tractive force F_{tr} is the product of torque T_{mot}, angular frequency ω, final gear drive ratio *G*, and wheel radius r_W minus the braking force F_b. The tractive force F_{tr} is subtracted by aerodynamic drag force F_{aero}, rolling resistance force F_{rr} and grade/slope force F_{grade} to inertial force F_i. The dependency of F_{aero} from the square of velocity *v* is not shown for reasons of clarity.

The inertial force F_i is the input for the proportional vehicle model that produces the output acceleration of the vehicle *a* which itself is integrated into velocity *v*, being fed back for comparison with trip driving cycles as the reference variable. Further, the velocity *v* is translated into motor speed *rpm* and angular frequency ω.

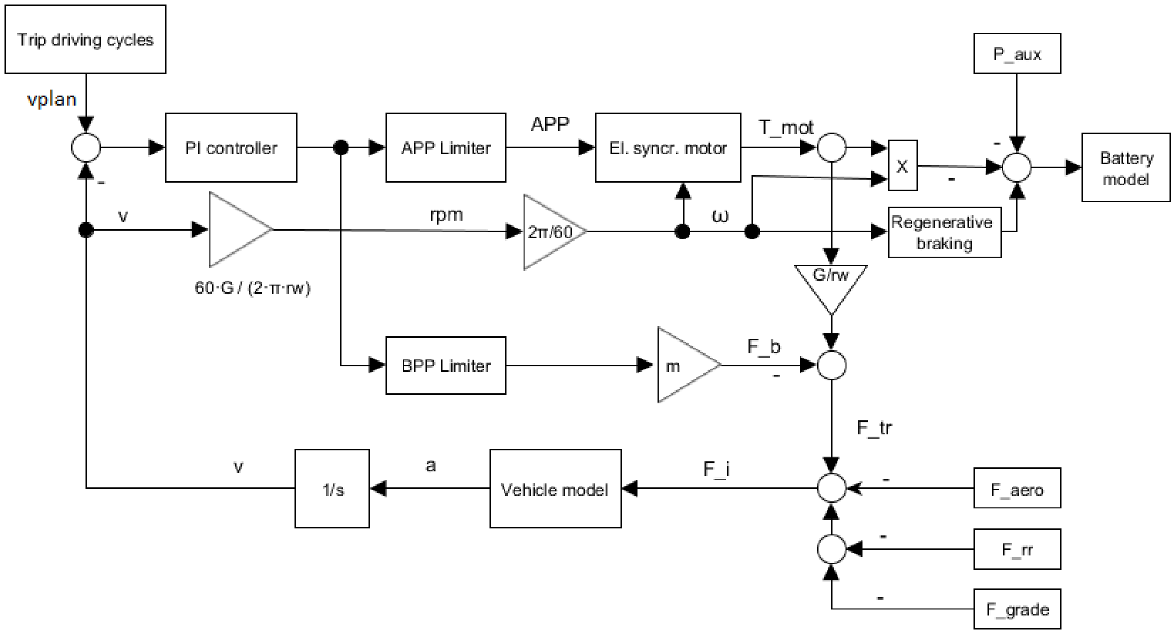

Figure 4 Schematic diagram of a principal bus vehicle model with electric drivetrain and battery model

The product of angular frequency ω and torque T_{mot} defines the required motor power input that is negatively fed into the battery model. Likeweise, negative auxiliary load P_{aux}, for accessories (HVAC etc.) is fed into the battery model, indicating the produced energy drain.

5.4 Regenerative braking

Regenerative braking stands for the recovery of kinetic energy and its conversion into electrical energy used for in-motion re-charging the battery, also denoted as battery recuperation. The input for regenerative braking model is the angular frequency ω to calculate the regenerative proportion of motor torque that is useable for recuperation.

Energy recovery is active only during braking commands of the “driver” in the form of the PI controller algorithm. Further, only a proportion of mechanical energy is converted into electrical energy, because the vehicle cannot be braked only by using the electric motor as generator. Hydraulic braking cylinders and metal discs are necessary to allow for emergency braking at any time. So, a significant share of kinetic energy is converted into thermal energy produced by friction forces applied to the braking discs.

In the simulated urban driving scenarios, it was estimated that approximately 50% of the kinetic energy is useable for battery recuperation.

The amount of energy used for recuperation was calculated by aggregating the portions of charging current towards the battery during braking manoeuvres. The ratio of the regenerative braking proportion to the energy consumed during recharging operations over a full day was determined to 55%, supporting the estimation. These results are compared to experimental results of an energy regeneration efficiency of 52-65%, according to [13].

5.5 Simulation design

For the simulation of a full-day revenue service cycle the basic transport task is described as:

a) Pull-out from depot to the nearer terminal stop of the transit route on the shortest path,

b) Round trip revenue route service between near and far terminal stop on the transit route including opportunity charging at the near terminal, and

c) Pull-in from near terminal stop to depot for servicing and overnight charging.

The vehicle driving cycle is simulated by means of a closed-loop discrete system of the vehicle model and a controller in a feedback loop. A proportional integral (PI)-controller is selected to simulate the acceleration and deceleration actions of the driver. The process variable of the control system is the velocity of the vehicle. The time/space-dependent value of the desired velocity is the variable, to be compared with the actual velocity, representing the error signal. The desired velocity alters according to the timetable of the vehicle. The PI controller attempts to minimize the error signal over time by adjustment of the control variable, namely the positive or negative acceleration of the vehicle. The desired velocity profile was measured during a route trip in the bus by GPS of a smartphone. Alternatively, if no GPS-tracks are available, this profile can be generated from GTFS data including the stop locations along the trip.

5.6 Scheduling and bus frequency

For the studied example case, the number of buses to deploy for the given route service is considered as constant because the headway of services is specified by the urban planning authority in the local public transport plan as a fixed requirement of the concluded entrustment agreement between municipality and transport agency. During peak hours from 7-9 a.m. and 2-5 p.m., the headway is planned as 10 minutes, resulting for the given one-way route length of 5.5 km in the need of 5 e-buses for a complete electrified route service.

5.7 Simulation experiments and results

Firstly, each bus cycle was simulated as a single trip between the two terminals of the given route, which consumes about 1.2 seconds CPU time. The total of 38 cycles over the full day, including pull-out trip, all 18 return trips between terminals and pull-in trip used about 45 seconds CPU time.

Figure 5 shows the simulation results of one single trip between terminal 1 and terminal 2. Chart A is the planned velocity v_{plan} in meters per second according the measured real-time field values displayed as the black line versus the simulated velocity v of the vehicle model, displayed by the green line. The latter simulated velocity shows a good alignment with the black real velocity, which suggests good tuned PI-controller variables with K_P = 0.15 and K_I = 0.01. A derivative controller term has been waived.

Furtherly indicates the match of curve shapes a realistic behaviour of the vehicle model including the drive train. In chart B is depicted the rotational speed ω of the electric motor shaft in radians per second as the purple line. The black line indicates the net motor torque T_{mot} in Newton meters including positive and negative values accounting for acceleration and deceleration manoeuvres.

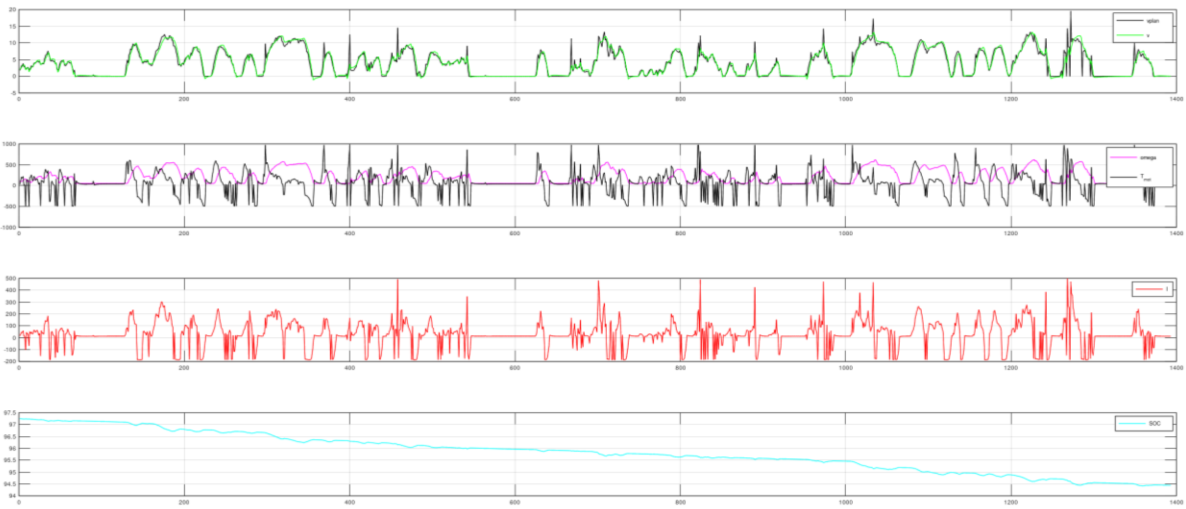

Figure 5 Simulation results of a single bus trip between terminal stops with real-time velocity data

Braking energy is represented by negative torque values, which is partially recuperated using the motor as generator for recharging the vehicle traction batteries. This effect is shown in chart C by the electric current I in Ampere that is simulated by calculating the electrical power output of the batteries, through open circuit voltage and internal resistance. Chart D displays the decrease of the State of Charge SOC in percent of the total battery capacity during the regarded trip from 97.2% to 94.5%. The difference of 2.7% for one trip, and respectively 5.4% for a round trip equals an energy consumption of 13 kWh.

Given the travelled distance of 11 km, the consumed energy per km is 1.18 kWh/km, which corresponds satisfactory well with field operational tests carried out with deployed battery electric buses in the Foothill study [10], (2.15 kWh/mile = 1.33 kWh/km). It should be noted that recuperation of the battery during negative current pikes is observed, leading to slightly increasing values in the SOC curve.

In Figure 6 is shown the complete simulation of a bus vehicle operation over a full day of revenue service with respect to State of Charge SOC. The simulation of SOC level is essential for dimensioning the battery size as the main factor of procurement cost. Starting point of a full day bus service is the depot at a SOC level of 100% after overnight slow charging. The pull-out distance from depot to the start terminal 1 of the route is approximately 3.8 km.

Terminal 1 is the starting point for the revenue service. Each return trip cycle has a distance of approximately 11 km. After 18 return trip cycles an opportunity charging [8] is carried out at terminal 1 where the charging facility shall be located. The fast charging process at half capacity ½C requires a power of 120 kW with a charging current of 200 A for the time of 300 seconds or 5 minutes.

The overall battery capacity of the bus is 240 kWh. An accessory load for heating, ventilation, air condition (HVAC) and auxiliary energy consumption such as power steering and door openers was approximated to 5 kW according to investigations of buses in real service, by Vepsäläinen [5]. The lowest value of SOC with 67% over the full day service was reached after the last duty cycle. The daily service is concluded by the pull-in trip into the depot where slow charging at 1/8 C is conducted. The overnight charging process requires a power of 30 kW with a charging current of 50 A for 2.4 hours.

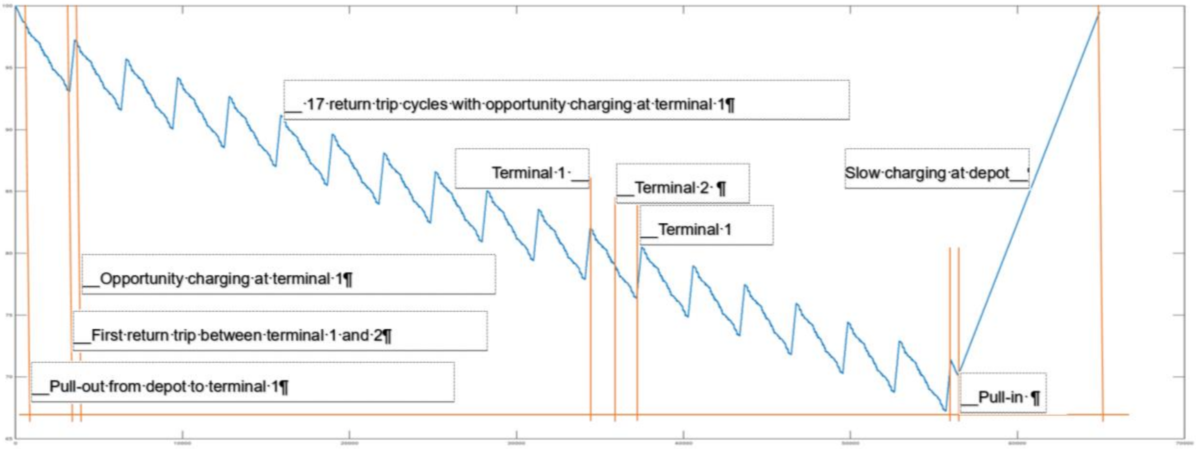

Figure 6 SOC over a full day including pull-out, 18 duty cycles, pull-in trip with overnight charging

The time interval of the SOC curve in Figure 6 is 65,149 seconds or 18.1 hours.

In the current state of the project work it can be confirmed that the developed simulation model and the simulation environment is well suited to support bus fleet electrification. Especially the dimensioning of battery sizes, estimation of energy demand, and localization of charging infrastructure can be achieved. By these factors an assessment of procurement costs can be supported in direct connection with the real bus route network to be designed. The results of the given analyses are subject to further input to assess life cycle costs and impacts as a base for procurement decisions by the corporate management of the public transport operator as suggested by Harris [7]. For the simulated and described use case scenario the following conclusions are drawn:

- The selected battery configuration allows for sufficient spare capacity that would allow deploying the bus/battery configuration for routes with trip lengths exceeding the considered one.
- The full day duty cycle is accomplished in 18 hours at a slow charging time in the depot of 2.4 hours, which leaves enough time for slow charging of more buses in the depot.
- The return trip travel time of 46 minutes including average dwell times in 10 trip stops of each 20 seconds allows for sufficient time for opportunity charging in one of the terminal stops.
- Consequently, an installation of an opportunity charging facility in one of the terminals is sufficient for the given route.

- The selected bus route appears well suited for electrification as the typical urban acceleration scenario allows for battery recuperation during deceleration maneuvers that relates to a higher Kinetic intensity, which is subject to further investigation.

The model was further extended to calculate quantities for an improved determination of the electrification-worthiness and duty cycle characterization of the bus route under examination. The metrics we used for assessment of the worthiness for electrification are *characteristic acceleration*, *aerodynamic speed*, and *kinetic intensity* and is to be referred in [6].

6 Simulation Model for the Monte Carlo optimization

In the course of the project work, modern data structures, database systems, data exchange software are used to achieve an efficient simulation environment. In the case that required data is not available or if its generation assumes employment of an analytical model of an unreasonable size, the data will be simulated by a random sampling technique similar to the Monte-Carlo method. In order to keep the simulation process fast, different time (or event) scales can be applied depending on the specific purpose of the dynamic process. If the process is a single bus run between two stations, then the time scale can be based on minutes or seconds, or even assuming continuous time. If the process includes all bus activities over a day, then it can be based on minutes or bus arrivals and departures from stations. The current chapter describes this approach in more detail by the example of determination of the most cost efficient charging strategy.

A model is developed to answer the question what recharging regime is more cost efficient

- Intermediate ultra-fast recharging (sharing infrastructure amongst multiple lines) or
- Final terminal recharging, having usually one recharging point per line

In practice the central hub is not a good place for recharging, since to many buses are circulating and space is limited. But under other circumstances it would be possible having single pole and transformers at each extreme position of the route. For circular routes it is possible defining one stop with a longer duration of the halt for having a buffer compensating delay. The Monte-Carlo (MC)-optimization should deliver a decision support, whether opportunity recharging at normal bus stops is generating enough savings to keep that variant in focus. Especially in growing cities terminal stops are moving, and thus the intermediate recharging should not be scrapped before detailed investigations. The calculation shall take all cost into consideration which are depending on the charging type.

- Battery lifetime depending on the C-rate for charging
- Charging infrastructure depending on directionality and charging power
- Grid access cost depending on charging power
- Charging losses depending on the C-rate for charging (Ohm's losses)

The C-rate is a quantification used for the maximum charging and discharging currents of a battery It is defined as the quotient of the maximum charging or discharging current and the capacity of the battery.

For longer charging times the driver may rest, but those efficiency gains with regards to mandatory pauses are not considered here. Not considered here are differing costs for erecting substations, since they are depicted in the grid access cost.

Most of the data are assumptions and need to be validated.

6.1 Implementation of the Monte-Carlo model

The flow diagram of the Monte-Carlo optimization model for the implementation is shown below in Figure 7.

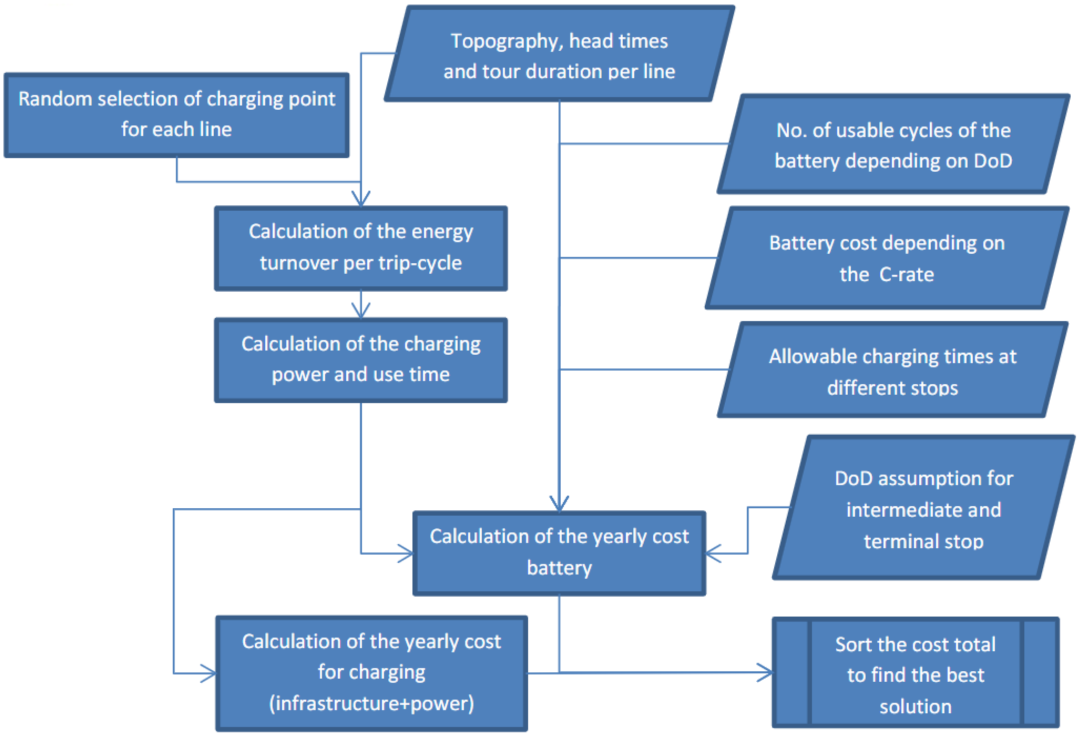

Figure 7 Flow diagram Monte Carlo optimization

The trip-cycle length is the distance driven between recharging stops. The assumption of the Depth of Discharge (DoD) has to be considering an optimum value, which heavily depends on the assumptions of the durability of the battery and the extra cost for battery chemistries allowing higher C-rates.

6.2 Cost of rechargeable batteries

The most important factor when determining the cost for rechargeable batteries is the length for the depreciation period. Servicing costs are neglected in this context. For the usable lifespan of the battery -expressed in full cycles - the depth of discharge (in the current case is considered the hourly swing) is the driving factor. Figure 8 shows the dependency derived from literature.

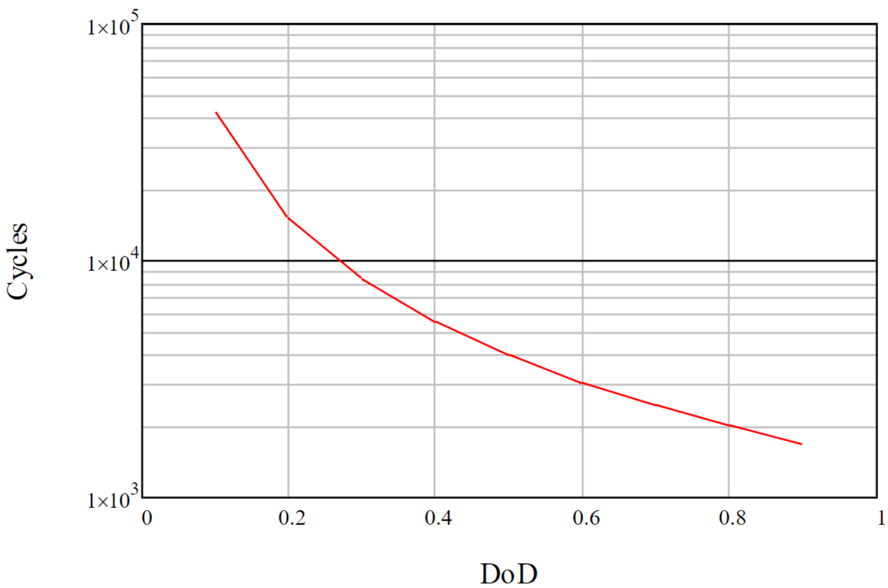

Figure 8 Number of usable cycles varying the depth of discharge (Hoke & Dragan Maksimovic, 2014 [14])

The second factor of influence for calculating the total cost of ownership is the C-rate. Rechargeable batteries allowing faster recharge are costlier. Cost correlation was derived from a scientific calculation of battery cost for different types of batteries, depending on the discharging rate, so the results have to be used cautiously. The assumption in the model is depicted in the following Figure 9.

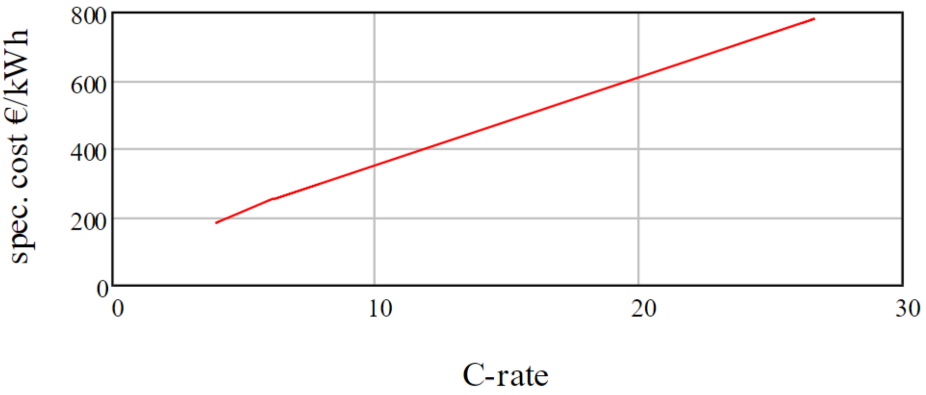

Figure 9 Specific battery cost depending on the discharging C-rate derived from (Nelson, Gallagher, Bloom, & Dees, 2011 [15])

For the Monte-Carlo variation, a minimum value for the specific cost has to be assumed. This is the value for 0.5 C. Also, the calendric lifespan (10 years was assumed) limits the number of cycles which might be achieved. Additionally, fixed integration cost of 50€ per kWh battery capacity have been assumed. Using those assumptions two typical curves for cost depending on the DoD are shown in Figure 10.

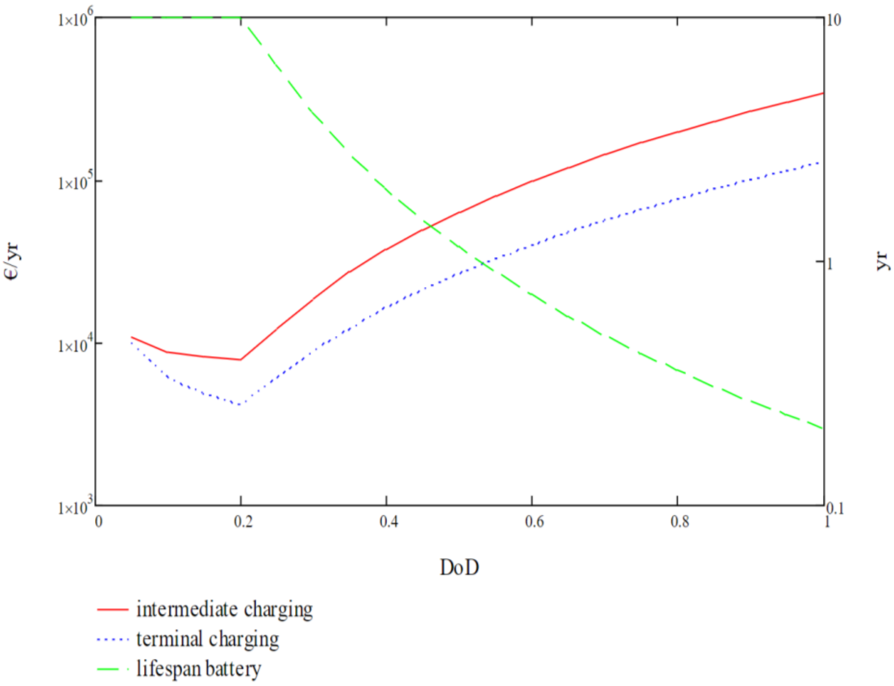

Figure 10 Optimal Depth of Discharge for two scenarios

The following Figure 11 shows the *MathCAD* coded subroutine for calculation of the battery total cost of ownership

.

$$
\mathrm{TCO\_Battery}(len, len_{ges}, t_{lade}, DoD, t_{tour}, t_{head}, b_{op}) :=
\left|
\begin{array}{l}
\text{"Energy demand"} \\
E_{trip} \leftarrow \mathrm{EnergyDemand}(len, len_{ges}) \\
P_{lade} \leftarrow \dfrac{E_{trip}}{t_{lade}} \\
a_{batlife} \leftarrow \mathrm{lifespan}_{bat}(E_{trip}, DoD, b_{op}, t_{tour}) \\
\mathrm{spur}\left(\text{"batlife=\{0\}"}, \dfrac{a_{batlife}}{Jahr}\right) \\
E_{bat} \leftarrow \dfrac{E_{trip}}{DoD} \\
C_{bat} \leftarrow \dfrac{P_{lade}}{E_{bat}} \\
cost_{el} \leftarrow p_{el} \cdot \dfrac{\dfrac{E_{trip}}{t_{tour}}}{eta_{charge}(C_{bat})} \cdot b_{op} \\
specCost \leftarrow \left[\left[\max\left(\begin{pmatrix} \mathrm{specAkkuCost}(C_{bat} \cdot h) \\ \mathrm{specAkkuCost}(0.5) \end{pmatrix}\right) + cost_{integr}\right] \cdot \dfrac{E_{bat}}{a_{batlife}} + cost_{el}\right] \cdot \mathrm{ceil}\left(\dfrac{h}{t_{head}}\right) \\
\text{return } specCost
\end{array}
\right.
$$

Figure 11 Subroutine calculation of battery cost

6.3 Recharging facility

The cost of the charging facility comprises three items:

- -Pole with contact, either wires or flat contact
- Cables connecting transformer and pole
- Transformer

For terminal stops only 10m cable instead of 20m and only one pole per stop was assumed. For shared intermediate stops, it was assumed that for each direction one pole is erected, and one transformer shared. Figure 12 shows the subroutine for calculating the cost of the recharging facility.

$cost_{fix} := 3200 \frac{€}{m}$ cables $\quad t_{d\_fix} := 25yr$ depreciation

$\_cost_{ch} := 5000 \cdot \frac{€}{kW}$ pole $\quad t_{d\_ch} := 20yr$ http://www.diva-portal.org/smash/get/diva2:967688/FULLTEXT01.pdf

$\_cost_{trafo} := 1600 \frac{€}{kW}$ trafo $\quad t_{d\_trafo} := 25yr$

$P_{0trafo} := 100 \cdot kW$ https://electrical-engineering-portal.com/price-of-a-transformer

$P_{0ch} := 400 \cdot kW \qquad cost_{trafo} := \_cost_{trafo} \cdot P_{0trafo} \qquad cost_{ch} := \_cost_{ch} \cdot P_{0ch}$

$$
\begin{aligned}
TCO\_ChargingInfra(len, len_{ges}, t_{lade}, t_{head}) := \;& E_{trip} \leftarrow EnergyDemand(len, len_{ges}) \\
& t_{use} \leftarrow \frac{t_{lade}}{t_{head}} \cdot Jahr \\
& p_{grid\_access} \leftarrow 70 \frac{€}{kW \cdot Jahr} \quad \text{if } t_{use} > 2500h \\
& p_{grid\_access} \leftarrow 15 \frac{€}{kW \cdot Jahr} \\
& P_{lade} \leftarrow \frac{E_{trip}}{t_{lade}} \\
& cost_{tr} \leftarrow cost_{trafo} \cdot \left(\frac{P_{lade}}{P_{0trafo}}\right)^{0.5} \\
& cost_{c} \leftarrow cost_{ch} \cdot \left(\frac{P_{lade}}{P_{0ch}}\right)^{0.4} \\
& spur(\text{"E.trip= \{0\} P.lade=\{1\}"}, E_{trip}, P_{lade}) \\
& C_i \leftarrow \left(\frac{cost_{ch}}{t_{d\_ch}} + \frac{cost_{trafo}}{t_{d\_trafo}}\right) + \frac{cost_{fix}}{t_{d\_fix}} \cdot 10m \quad \text{if } len = 0m \lor len = len_{ges} \\
& C_i \leftarrow \left(\frac{2 \cdot cost_{ch}}{t_{d\_ch}} + \frac{cost_{trafo}}{t_{d\_trafo}}\right) + \frac{cost_{fix}}{t_{d\_fix}} \cdot 20m \quad \text{otherwise} \\
& \text{"at end points there is only one pole- for 10 min head time"} \\
& \text{return } (C_i + p_{grid\_access} \cdot P_{lade})
\end{aligned}
$$

Figure 12 Subroutine for calculating the charging infrastructure cost

Since costs for the recharging infrastructure are shared amongst the circulating buses, the total cost for all bus batteries had to be taken into account. For each line ahead time, a yearly operation time and a total trip time between the recharging stops have been assumed. This fits perfectly the Monte-Carlo approach, since less productive charging stations are omitted automatically.

6.4 Potential improvements discussed

This is no simulation of the real operation, the charging times for opportunity charging are assumed according to times seen in practice (Demonstrators in Graz), and might be adapted to see the sensitivity. Costs for accessing the grid are included in the model, but the use time of the station is not accumulated yet, taking more bus lines together. Same applies for multiple stops per line which are not considered so far as potential solution, but should now.

Also, additional battery weight is left out which might increase the energy demand. Sharing the infrastructure cost amongst lines is modelled taking the together the number of circulating buses at the specific intervals. Having only one pole per stop intermediate recharging suffers from the problem that two buses might arrive at the same time at the recharging stop. This problem might occur more often if the head times are equal. Further investigations are necessary; also producer of catenary type recharging stations might offer the benefit of allowing parallel recharging of two vehicles having different length.

6.5 Conclusion of the presented MC-optimization

Based on the assumptions for the recharging infrastructure and constructing a virtual network having some stops on also a terminal stop in common, the following recharging stations are causing the least cost, illustrated in Figure 13.

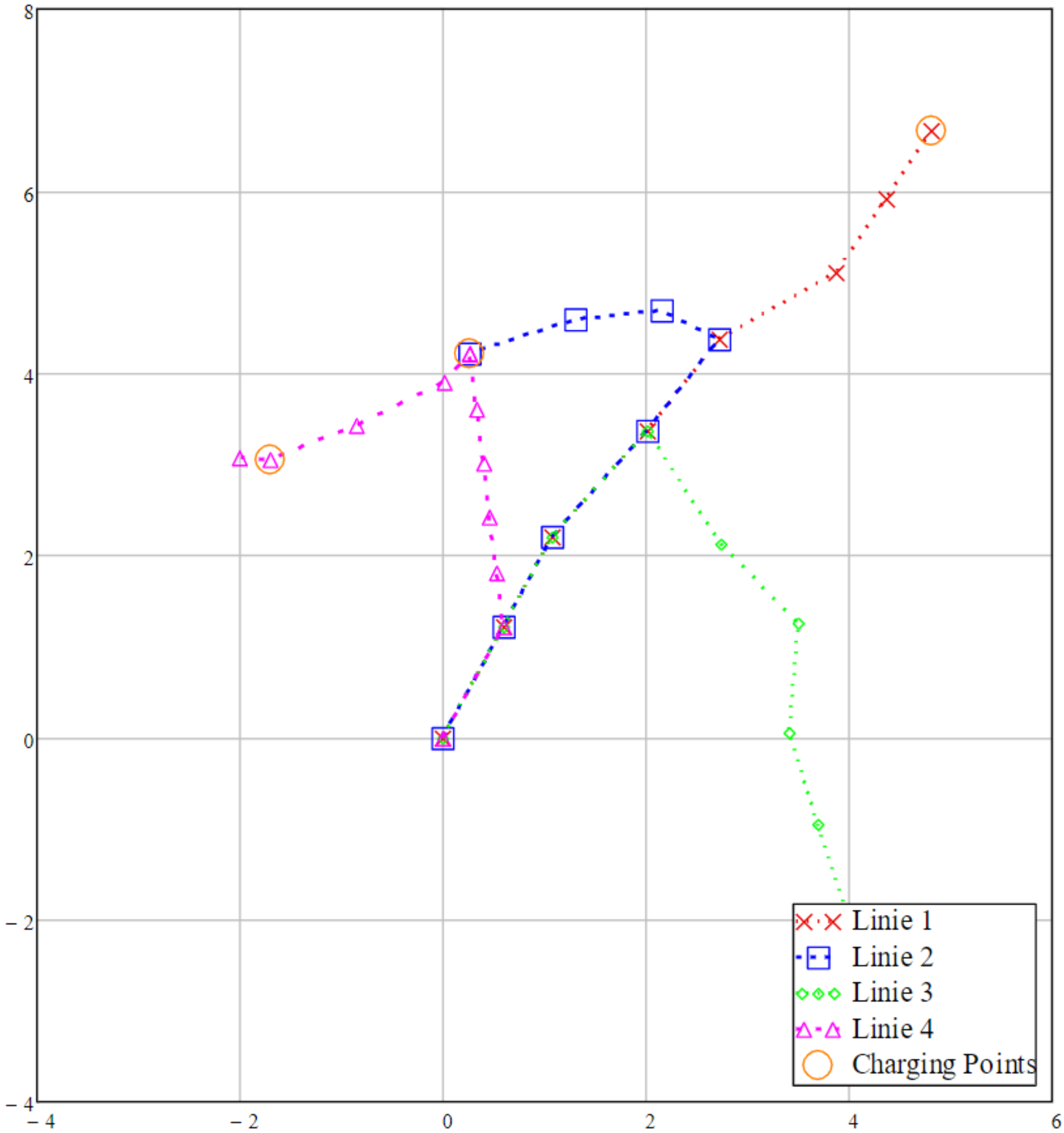

Figure 13 Map of the virtual bus network, showing recharging points

It is noticeable that only three recharging stops are needed, where one is positioned at the terminal stop and one shared heavily. Potential conflicts are not depicted by the model.

The sorted cost curve is depicted below in Figure 14. Although 10^6 variants were calculated, the Monte Carlo approach might miss the optimum. This is very much depending also on the quality of the random number generator.

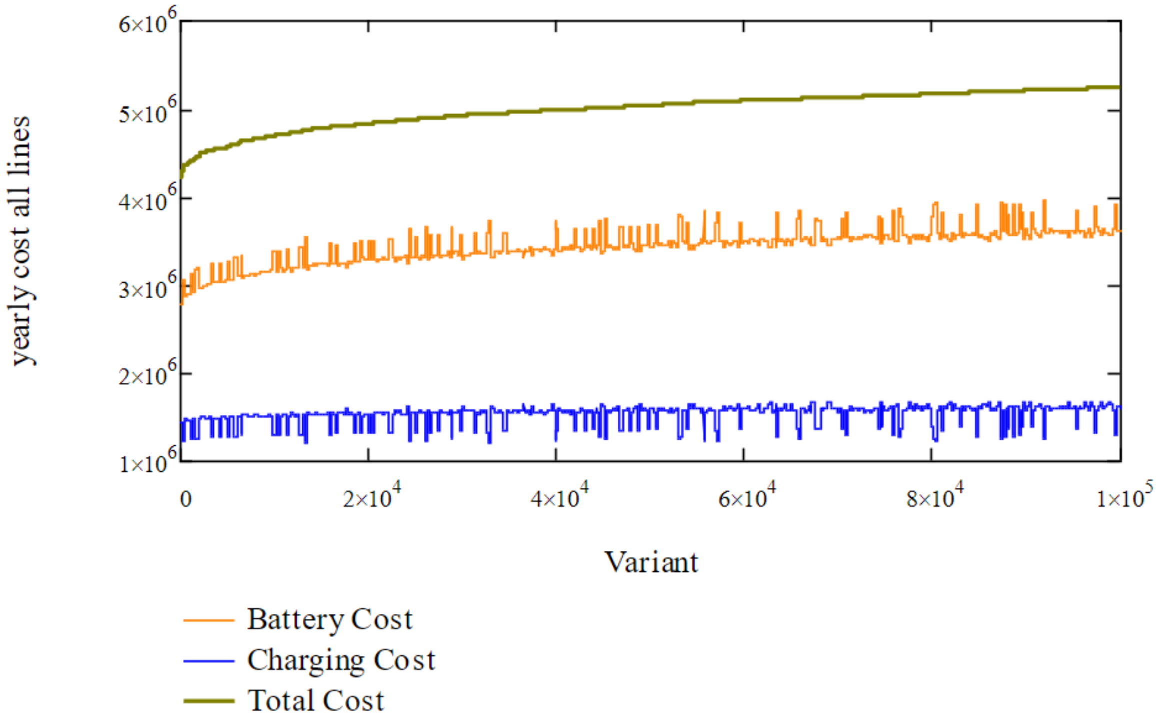

Figure 14 Sorted total cost curve of the best 10^5 MC-variants

6.6 Discussion of the results of the MC-optimization

An extended optimization approach would also vary DoD and recharging time and calculate the change in the occupancy rate. Unfortunately, there is no empirical data how passengers react to the variation of the recharging regime, having more or less waiting time.

Some observations in Graz may lead to the conclusion, that users of public transport having their mobile phones at hand and used to wait for several minutes at bus stops do not care that much about short halts, although operators tend to avoid still stands at stops, also because they are blocking the following buses.

Therefore, a simulation using real time data would be needed to determine the minimum battery size, because recharging often does not happen like planned. In the MC-variation the redundancy of the charging regime is high, since the assumption of the Depth of Discharge allows some tours without recharging.

But the optimum DoD is low and this optimization has to be challenged. With the data used, it might well be the case that minimizing battery size is not possible, since very small DoDs are favorable in terms of cost. This would also mean that deviations in actual charging times are less critical.

7 References

1. VDV Schriften 452 3/08, (2008). *ÖPNV Data Model 5.0, VDV Standard Interface Network/Timetable*, Version 1.4, Köln: Verband Deutscher Verkehrsunternehmen (VDV).
2. General Transit Feed Specification Reference (2015), https://developers.google.com/transit/gtfs/reference .
3. Algin, V.; Czogalla, O.; Kovalyov, M.; Krawiec, K.; Chistov, S.: *Essential functionalities of ERA-NET Electric Mobility Europe Platon project*, Mechanics of Machine, Mechanisms and Materials No. 4 (45), ISSN 1995-0470, 2018. Pages 17-28.
4. Sun, Zongxuan, and Guoming Zhu (2015): *Design and control of automotive propulsion systems. Boca Rota*, FL Tylor & Francis Group LLC, CRC Press, 2015.
5. Vepsäläinen, J; et. al (2018): *Energy Uncertainty Analysis of Electric Buses, Multidisciplinary Digital Publishing Institute*, MDPI Journal of Energies 2018, 11, 3267, doi:10.3390/en11123267, Basel
6. O'Keefe, M; Simpson, A.; Kelly, K. (2007): *Duty Cycle Characterization and Evaluation Towards Heavy Hybrid Vehicle Applications*. SAE World Congress and Exhibition, April 16-19, 2007, Detroit, Michigan.
7. Harris, A; Soban, D.; Smyth, B.: Best, R. (2018): *Assessing life cycle impacts and the risk and uncertainty of alternative bus technologies*, J Renewable and Sustainable Energy Reviews 97 (2018), 569-579 Elsevier.
8. Kunith A, Mendelevitch R, Goehlich D.: *Electrification of a city bus network - An optimization model for cost-effective placing of charging infrastructure and battery sizing of fast charging electric bus systems*. Int J Sustain Transp 2017;11:707–20.
9. LowCVP. *Low Emission Bus Testing Guidance for test houses*; 2015.
10. Eudy, L; Prohaska R.; Kelly K.; Post, M. (2016): *Foothill Transit Battery Electric Bus Demonstration Results*, National Renewable Energy Laboratory, Technical report NREL/TP-5400-65274, Denver, January 2016.
11. Schaltz, Erik: *Vehicle Energy Consumption,* Online available at http://www.risoe.dk/rispubl/NEI/NEI-DK-5575.pdf
12. UITP (2014) UITP SORT Brochure (2014): *E-SORT–Standardised On Road Test Cycles for electric buses*. International Association of Public Transport, Brussels 2014.
13. Zhang, J.; Lu, X.; Xue, J.; and Li, B.: *Regenerative braking system for series hybrid electric city bus*, The World Electric Vehicle Journal, vol. 2, no. 4, 2008.

14. Hoke, A., &Dragan Maksimovic, A. P. (2014). *Accounting for Lithium-Ion Battery Degradation in Electric Vehicle Charging Optimization*. JESTPE 2013.

15. Nelson, P., Gallagher, K., Bloom, I., & Dees, D. (2011). *Modeling the Performance and Cost*. Oak Ridge: Argonne National Laboratory.